A new qualitative control strategy for the genetic Toggle Switch

Lucie Chambon, Jean-Luc Gouzé

A new qualitative control strategy for the genetic Toggle Switch ⋆

Lucie Chambon * **Jean-Luc Gouzé** **

* *Université Côte d'Azur, Inria, INRA, CNRS, Sorbonne Université, Biocore Team, Sophia Antipolis, France (e-mail: lucie.chambon@inria.fr)*
** *Université Côte d'Azur, Inria, INRA, CNRS, Sorbonne Université, Biocore Team, Sophia Antipolis, France (e-mail: jean-luc.gouze@inria.fr)*

Abstract: Genetic positive feedback loops are essential for cell decision making and cell differentiation. They are traditionally described by a two-dimensional smooth non-linear differential system composed of Hill functions. The bistability of this classic model properly captures the decision properties of these biological motifs. This paper designs a new control strategy based on the measurement and control of a unique gene within the loop, in order to stabilize the system around its unstable fixed point. The quantized nature of genetic measurements and the new synthetic control approaches available in biology encourage the use of a piecewise constant control law. A specific partitioning of the state space and the study of successive repelling regions allow to prove global convergence and global stability for the resulting system. The same strategy is shown to be efficient as well in the more realistic context in which measurements are considered possibly uncertain. This new control strategy is compared with a real biological experiment that was implemented for the Toggle Switch with the same stabilization objective, but for which both genes were measured and controlled.

Keywords: Gene regulatory networks; Qualitative control; Non-linear systems; Quantized measurements; Global stability.

1. INTRODUCTION

Gene regulatory networks have attracted a lot of interest in recent years due to the central role they play in any cell's function. Despite their complexity, few recurrent genetic motifs were found to be essential for many biological behaviors. This is the case of positive feedback loops. These building blocks are generally composed of genes that activate their own production directly or indirectly through other genes. Their presence is commonly associated with bistability or multistability, necessary for cell decision making and cell differentiation (Gardner et al., 2000).

Cell differentiation is the process during which a less specialized cell may change into a more specialized cell. An undifferentiated cell that is able to specialize into any specific cell is called a stem cell. These cells are extremely promising for medical treatments advances as they may replace any damaged cells. Furthermore, it has been shown recently that cell differentiation is a reversible process (Cai et al., 2007): scientists have been able to turn a differentiated cell back into an undifferentiated stem cell. This last observation provides evidence that understanding positive feedback loops mechanisms and finding tools to control them is of high interest.

To that end, synthetic biology has made significant progress over the past few years and has offered multiple tools for the design and the control of genetic motifs (Purcell et al., 2010). As a successful example, Gardner and Collins have synthetically constructed the first Toggle Switch in the organism *Escherichia Coli* (Gardner et al., 2000). This motif was composed of two genes *lacI* and *tetR* that mutually repressed each other through the proteins LacI and TetR for which they code. This circuit presented two stable states and an unstable state: from an undifferentiated state, cells eventually converged towards one of the two stable states. The use of both inducer molecules IPTG and aTc allowed to switch from one to the other. Very recently, Lugagne et al. (2017) achieved to reverse the decision process: the cells were forced to converge towards the unstable fixed point. This objective was achieved by measuring and controlling both genes. The level of expression of *lacI* and *tetR* was estimated with fluorescent microscopy techniques, by measuring levels of two fluorescent proteins: RFP and GFP. These measurements affected microfluidics devices behaviors: the inhibition of *lacI* was dynamically controlled by aTc and *tetR* by IPTG.

For both previous examples, mathematical modeling and the theory of dynamical systems and control may give a good insight on the system dynamics and help designing a first draft of a control strategy. However, due to several

⋆ This work was supported by Région PACA and by the French Government (National Research Agency, ANR) through the "Investments for the Future" LABEX SIGNALIFE: program reference ANR-11-LABX-0028-01.

biological constraints, classic models and mathematical tools are not relevant. Firstly, biological measurement techniques such as fluorescent microscopy, as introduced just before, prevent the use of classic control laws that depend on continuous and smooth observations of the variables. Indeed, in a genetic context the observation of each gene provides qualitative data due to the sensitivity of measurement techniques: as an example, a gene may be fully expressed or not expressed at all. Secondly, the control techniques usually available in biology provide constant outputs: this is the case for example with the introduction of specific doses of inducer molecules (Fracassi et al., 2015), or even with new optogenetic techniques that behave as on-off controllers (Milias-Argeitis et al., 2016). Finally these two biological realities encourage the use of piecewise constant control laws. These discontinuous models have been extensively used to model life, in neuroscience (Brette and Gerstner, 2005) or genetics (Chaves and Gouzé, 2011) to name but a few. The discontinuities that appear in these models have imposed the development of new analytical tools in order to tackle classic problems such as convergence (Farcot and Gouzé, 2009) or stability (Casey et al., 2006).

In this context, this article presents a new quantized control strategy for a two dimensional non-linear model of positive feedback loops, that measures and controls a unique gene within the loop in order to globally stabilize its unstable fixed point. The work will focus on the comparison between this new control approach and the biological control implemented by Lugagne et al. (2017) that was introduced earlier. In this latter experiment, both genes *lacI* and *tetR* were measured and controlled. From a mathematical point of view, this system is always controllable and it is a lot more challenging to control and measure only one gene. From a biological point of view, the present study aims to reduce measurement devices by using a unique fluorescent protein (GFP) and facilitate control implementation by introducing a unique inducer molecule (aTc).

Section 2.1 presents the general two-dimensional non-linear model for positive feedback loops. In this framework, the calibration of the Toggle Switch used in Lugagne et al. (2017) is introduced in Section 2.2 and will allow several comparisons through the whole paper between the new control strategy and their control implementation. The design of the new control strategy is presented in Section 3, and the resulting global properties are proved in Section 4: global attractivity is first verified by constructing successively repelling regions of the state space, and robustness is established through Lyapunov stability. In a more realistic context where measurements can be uncertain, it is shown in Section 5 that the same control strategy guarantees global convergence in a small zone around the unstable fixed point.

2. THE UNCONTROLLED SYSTEM

2.1 The model

With two components, positive feedback loops have been commonly modeled by two coupled non-linear differential equations (Lugagne et al., 2017):

$$\begin{aligned}\dot{x}_1 &= \kappa_{01} + \kappa_1 \mathrm{h}^-(x_2, \theta_2, n_2) - \gamma_1 x_1,\\ \dot{x}_2 &= \kappa_{02} + \kappa_2 \mathrm{h}^-(x_1, \theta_1, n_1) - \gamma_2 x_2,\end{aligned} \tag{1}$$

where $\mathrm{h}^-(x, \theta, n) = \theta^n/(x^n + \theta^n)$ is a decreasing sigmoid, called Hill function. This type of function is extensively used in genetics as it models the influence of a transcription factor on the expression of a gene. The parameter n represents the number of binding sites on the promoter and parametrises the steepness of the function, and θ represents the sensitivity of the feedback and parametrises the threshold of the function. For $i \in \{1, 2\}$, the parameters $\kappa_{0i} > 0$ model the basal production, $\kappa_i > 0$ the intensity of the interactions, and $\gamma_i > 0$ the degradation speed. As Hill functions are in the interval $]0, 1]$, it is easy to show that the trajectories of this system are bounded: for $i \in \{1, 2\}$, $x_i \in]\kappa_{0i}/\gamma_i, (\kappa_{0i} + \kappa_i)/\gamma_i]$. For a typical illustration with two genes, see Fig. 1.

As the composition of two Hill functions is still a sigmoid, it is possible to show that this loop has either a unique globally asymptotically stable fixed point or three fixed points depending on the parameters. In this second scenario, the analysis of the Jacobian matrix reveals two locally stable fixed points $\bar{x}_{inf}$ and $\bar{x}_{sup}$, and a last locally unstable fixed point $\bar{x}$ (see Fig. 3). Again, bounds on the fixed points are obtained: if x is a fixed point of (1), then for $i \in \{1, 2\}$, $x_i \in]\kappa_{0i}/\gamma_i, (\kappa_{0i} + \kappa_i)/\gamma_i[$. For the result on the upper bound, it is possible to show that if there exists $i \in \{1, 2\}$ such that $x_i = (\kappa_{0i} + \kappa_i)/\gamma_i$, then $x_i = 0$ $\forall i \in \{1, 2\}$ leading to $\kappa_{0i} = \kappa_i = 0$ $\forall i \in \{1, 2\}$, which is not allowed in our model.

With three fixed points, the model recovers the properties of positive feedback loops explained in the introduction: from an undifferentiated state, represented by the unstable fixed point $\bar{x}$, a cell might differentiate into one type or another type through a convergence towards one of the two stable fixed points. Hereafter, the parameters of (1) are assumed to generate three fixed points.

2.2 A comparative example: the Toggle Switch

Although the results presented in this article are valid for any parameters of (1), they will be illustrated in each section with a calibration of the Toggle Switch introduced in Lugagne et al. (2017). As explained in the introduction, their goal was to maintain the network near the unstable fixed point by measuring and controlling both genes with IPTG and aTc. In this present paper, the control technique will be reduced to the measurement and control of only one gene. The resulting strategy will be applied to a calibration of their system in order to allow constructive comparisons between both control processes. With the classic hypothesis that mRNA degrades faster than proteins, their 4-dimensional model can be reduced to (1) where $x_1 = \mathrm{LacI}$ and $x_2 = \mathrm{TetR}$. The uncontrolled Toggle Switch in Lugagne et al. (2017) was obtained under reference conditions $\mathrm{aTc}_{ref} = 20\mathrm{ng} \cdot \mathrm{ml}^{-1}$ and $\mathrm{IPTG}_{ref} = 0.25\mathrm{mM}$. Thus, the calibration is obtained for a rescaled system: $\dot{x}_1 = \kappa_{01} + \kappa_1 \mathrm{h}^-(u_1 x_2, \theta_2, n_2) - \gamma_1 x_1$ and $\dot{x}_2 = \kappa_{02} + \kappa_2 \mathrm{h}^-(u_2 x_1, \theta_1, n_1) - \gamma_2 x_2$ where $u_1 = \theta_{\mathrm{aTc}}^{\eta_{\mathrm{aTc}}}/(\theta_{\mathrm{aTc}}^{\eta_{\mathrm{aTc}}} + \mathrm{aTc}_{ref}^{\eta_{\mathrm{aTc}}}) \approx 0.25$ and $u_2 = \theta_{\mathrm{IPTG}}^{\eta_{\mathrm{IPTG}}}/(\theta_{\mathrm{IPTG}}^{\eta_{\mathrm{IPTG}}} + \mathrm{IPTG}_{ref}^{\eta_{\mathrm{IPTG}}}) \approx 0.12$. The parameters γ_1, γ_2, n_1, n_2,

θ_{aTc}, η_{aTc}, θ_{IPTG}, and η_{IPTG} were directly taken from their supplementary information, and the remaining six parameters were computed in order to get the same three fixed points. Parameters values are merged in table 1.

Table 1. Calibration parameters of the Toggle Switch based on Lugagne et al. (2017) data

κ_{01}	κ_1	θ_2	n_2	γ_1	θ_{aTc}	η_{aTc}
1.56	61.7	34.2	2	0.0165	11.65	2
κ_{02}	κ_2	θ_1	n_1	γ_2	θ_{IPTG}	η_{IPTG}
1.47	17.6	42.1	2	0.0165	0.0906	2

3. THE CONTROL

The suitable control must lead to a global convergence of the trajectories towards the unstable fixed point $\bar{x}$ of (1). Moreover, as explained in the introduction, the control strategy cannot depend precisely on the variables as measurements are of qualitative nature in biology. This biological reality justifies the use of piecewise constant control laws that depend on regions of the state space. Finally, in order to reduce measurement devices and facilitate implementations, only the first gene is measured and controlled. In this context, the controlled system becomes:

$$\begin{aligned} \dot{x}_1 &= \kappa_{01} + \kappa_1 h^-(u(x_1)x_2, \theta_2, n_2) - \gamma_1 x_1, \\ \dot{x}_2 &= \kappa_{02} + \kappa_2 h^-(x_1, \theta_1, n_1) - \gamma_2 x_2, \end{aligned} \tag{2}$$

with $u(x_1) = u_{min} < 1$ if $x_1 \leq \bar{x}_1$ and $u(x_1) = u_{max} > 1$ if $x_1 \geq \bar{x}_1$. This control strategy is adapted to quantized measurements available for the first gene: if x_1 is weakly expressed ($x_1 \leq \bar{x}_1$) the control decreases the influence of x_2 on x_1, and if x_1 is highly expressed ($x_1 \geq \bar{x}_1$), the control increases the influence of x_2 on x_1. The control $u(x_1)$ appears in the Hill function because it is considered that the control element is able to facilitate or prevent the second protein from binding to the promoter of the first gene. This hypothesis was also made in Lugagne et al. (2017), facilitating once again later comparison. For the Toggle Switch, such control can be performed with the inducer molecule aTc: the control condition $u_{max} > 1$ (resp. $u_{min} < 1$) results in increasing above (resp. reducing below) $20\text{ng} \cdot \text{ml}^{-1}$ the dose of aTc (see Fig. 1).

Next section states and proves global results about convergence and stability.

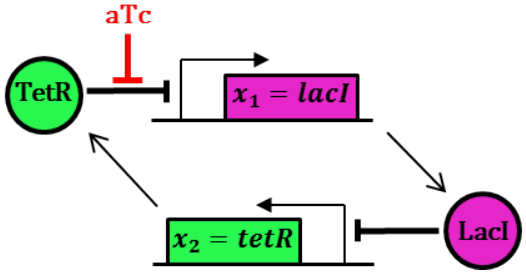

Fig. 1. Illustration of the Toggle Switch and aTc control strategy

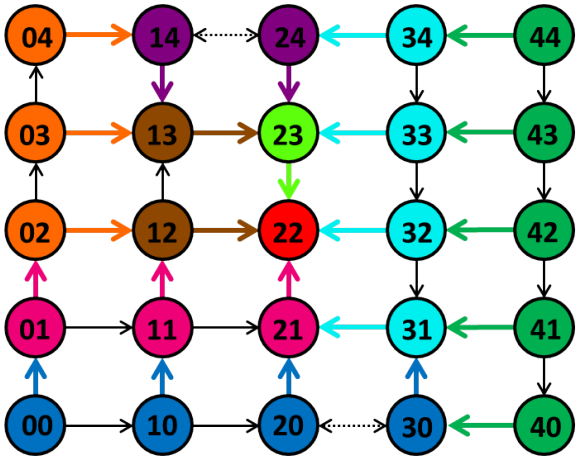

Fig. 2. Partitioning of the state space according to Definition 1. The arrows represent transitions between zones. Some transitions represented by the black arrows do not play any role in Lemma 3, and dashed black arrows illustrate unknown transitions. The successive repelling regions are represented with different colors and illustrate the repelling order given in Lemma 3.

4. GLOBAL RESULTS

In this section, appropriate conditions on u_{min} and u_{max} are determined in order to make $\bar{x}$ globally asymptotically stable. The state space is partitioned in 5^2 zones called $(a_1 a_2)$:

Definition 1. For $i \in \{1, 2\}$:

- $a_i = 0$ if $x_i < \bar{x}_i - \alpha_i$,
- $a_i = 1$ if $\bar{x}_i - \alpha_i \leq x_i < \bar{x}_i$,
- $a_i = 2$ if $x_i = \bar{x}_i$,
- $a_i = 3$ if $\bar{x}_i < x_i \leq \bar{x}_i + \beta_i$,
- $a_i = 4$ if $\bar{x}_i + \beta_i < x_i$,

where:

- $\beta_1 = (\kappa_{01} + \kappa_1)/\gamma_1 - \bar{x}_1$,
- $\alpha_2 = \bar{x}_2 - \frac{\kappa_{02} + \kappa_2 h^-(\bar{x}_1 + \beta_1, \theta_1, n_1)}{\gamma_2}$,
- $\alpha_1 = \bar{x}_1 - \kappa_{01}/\gamma_1$,
- $\beta_2 = \frac{\kappa_{02} + \kappa_2 h^-(\bar{x}_1 - \alpha_1, \theta_1, n_1)}{\gamma_2} - \bar{x}_2$.

It is easy to show that $\forall i \in \{1, 2\}$, $\alpha_i > 0$, $\beta_i > 0$, and $\alpha_i < \bar{x}_i$. Moreover, the central zone $(2, 2)$ is the fixed point $\bar{x}$. An illustration of this partitioning is presented as a graph in Fig. 2.

This partitioning allows the statement of the first main result of this paper:

Theorem 2. With $u_{min} \leq \bar{x}_2/(\bar{x}_2 + \beta_2)$ and $u_{max} \geq \bar{x}_2/(\bar{x}_2 - \alpha_2)$, (2) converges globally towards $\bar{x}$.

With the properties of Hill functions, it is easy to check that $u_{min} < 1$ and $u_{max} > 1$. The proof of this theorem is built by studying successively repelling regions of the state space. The general idea is the following: a region, defined as a union of zones $(a_1 a_2)$, is repelling in direction i if the vector field $\dot{x}_i$ keeps a constant sign in the whole region. If $\dot{x}_i > 0$ (resp. < 0), the trajectories will leave the region

through the upper (resp. lower) bound defining a_i, as all regions are bounded in this problem. This idea leads to the following Lemma:

Lemma 3. These specific regions are successively repelling:

(1) The region $a_1 = 4$ is repelling.
(2) If the region $a_1 = 4$ is repelling, then the region $a_2 = 0$ is repelling as well.
(3) If the region $a_2 = 0$ is repelling, then the region $a_1 = 3$ is repelling as well.
(4) If the regions $a_1 = 4$ and $a_1 = 3$ are repelling, then the region $a_2 = 1$ is repelling as well.
(5) The region $a_1 = 0$ is repelling.
(6) If the region $a_1 = 0$ is repelling, then the region $a_2 = 4$ is repelling as well.
(7) If the region $a_2 = 4$ is repelling, then the region $a_1 = 1$ is repelling as well.
(8) If the regions $a_1 = 0$ and $a_1 = 1$ are repelling, then the region $a_2 = 3$ is repelling as well.

This Lemma allows the construction of Theorem 2.

Finally, the trajectories globally converge towards $\bar{x}$ through a sliding mode on the line $x_1 = \bar{x}_1$. A summary of this result is illustrated by a transition graph in Fig. 2.

The second main result states the stability of $\bar{x}$:

Theorem 4. With $u_{min} < 1$ and $u_{max} > 1$, $\bar{x}$ is Lyapunov stable.

The conditions on u_{min} and u_{max} given in Theorem 4 are relaxed compared to the one given in Theorem 2. Indeed, if u_{min} and u_{max} are not small and large enough, $\bar{x}$ becomes locally stable through a sliding mode. However, $\bar{x}_{inf}$ and $\bar{x}_{sup}$ are still present and stable as well, preventing global convergence towards $\bar{x}$.

In order to verify the classic definition of Lyapunov stability, the proof uses the construction of specific squares and rectangles: for any square $\mathcal{B}_\delta = \{x| \, ||x(t) - \bar{x}||_\infty \leq \delta\}$ of length $\delta > 0$ centered on $\bar{x}$, an invariant rectangle $\mathcal{B}$ centered on $\bar{x}$ can be constructed such that $\mathcal{B} \subset \mathcal{B}_\delta$. Finally this rectangle $\mathcal{B}$ is restricted to a square of initial conditions of length $\epsilon > 0$ called $\mathcal{B}_\epsilon = \{x| \, ||x(t) - \bar{x}||_\infty \leq \epsilon\}$ centered on $\bar{x}$.

Initially, the length δ is restricted to Assumption 5:

Assumption 5. $\forall i \in \{1, 2\}$ the length δ verifies: $\delta < \min\left(\bar{x}_i - \kappa_{0i}/\gamma_i, (\kappa_{0i} + \kappa_i)/\gamma_i - \bar{x}_i\right)$.

With boundedness properties of (1), it is possible to find such a $\delta > 0$. From the corresponding square $\mathcal{B}_\delta$, the invariant rectangle $\mathcal{B}$ can be constructed:

Definition 6. For a fixed $\delta > 0$ under Assumption 5, the region $\mathcal{B}$ is defined with:

- $\mu_2 = \min\left(\delta, x_{2max}\right)$ and $M_2 = \mu_2$,
- $\eta_1 = \bar{x}_1 - \mathrm{h}_2^{-1}\left(\frac{\gamma_2(\bar{x}_2 + M_2) - \kappa_{02}}{\kappa_2}\right)$ and $m_1 = \min\left(\delta, \eta_1\right)$,
- $\eta_2 = \min\left(\delta, x_{2min}\right)$ and $m_2 = \eta_2$,
- $\mu_1 = \mathrm{h}_2^{-1}\left(\frac{\gamma_2(\bar{x}_2 - m_2) - \kappa_{02}}{\kappa_2}\right) - \bar{x}_1$ and $M_1 = \min\left(\delta, \mu_1\right)$,

where $x_{2max} = \bar{x}_2/u_{min}$ is the intersection between the x_1-nullcline in the space $x_1 < \bar{x}_1$ and the line $x_1 = \bar{x}_1$, $x_{2min} = \bar{x}_2/u_{max}$ is the intersection between the x_1-nullcline in the space $x_1 > \bar{x}_1$ and the line $x_1 = \bar{x}_1$, and h_2^{-1} is the inverse function of $\mathrm{h}^-(x_1, \theta_1, n_1)$.
Then $\mathcal{B} = \{x | \bar{x}_i - m_i \leq x_i \leq \bar{x}_i + M_i \quad \forall i \in \{1, 2\}\}$.

It is easy to check that $\forall i \in \{1, 2\}$ $\bar{x}_i < \bar{x}_i + M_i < (\kappa_{0i} + \kappa_i)/\gamma_i$, $\kappa_{0i}/\gamma_i < \bar{x}_i - m_i < \bar{x}_i$, and $\mathcal{B} \subset \mathcal{B}_\delta$. It is possible to prove that the rectangle $\mathcal{B}$ is invariant:

Lemma 7. For any initial condition $x(0) \in \mathcal{B}$, $x(t) \in \mathcal{B}$ for any $t \geq 0$.

To prove this Lemma, it is shown that the vector field in the perpendicular direction of each of the four boundaries of rectangle $\mathcal{B}$ points inward. The length ϵ of the last square $\mathcal{B}_\epsilon$ is now introduced:

Definition 8. For a fixed $\delta > 0$ under Assumption 5, $\epsilon = \min\left(\min_i m_i, \min_i M_i\right)$.

Basically, the square $\mathcal{B}_\epsilon$ is the restriction of rectangle $\mathcal{B}$ to its biggest embedded square.

Remark 9. If Assumption 5 is not fulfilled for a $\delta > 0$, then it is sufficient to consider any square of length $\delta' > 0$ such that $\mathcal{B}_{\delta'} \subset \mathcal{B}_\delta$ and such that δ' fulfills Assumption 5. The rectangle $\mathcal{B}$ is constructed for $\mathcal{B}_{\delta'}$, as well as the initial condition square $\mathcal{B}_\epsilon$.

All these Lemmas, Definitions and Remarks introduce the final proof for Theorem 4:

Proof. For any $\delta > 0$, there exists an $\epsilon > 0$, as stated in Definition 8 and Remark 9, such that every solution $x(t)$ having initial conditions in the square $\mathcal{B}_\epsilon$ (i.e. within a distance ϵ of the equilibrium: $||x(0) - \bar{x}||_\infty \leq \epsilon$), remains in the rectangle $\mathcal{B}$ as stated by Lemma 7. As $\mathcal{B} \subset \mathcal{B}_\delta$, the trajectories stay in $\mathcal{B}_\delta$ (i.e. within a distance δ of the equilibrium: $||x(t) - \bar{x}||_\infty \leq \delta$) for all $t \geq 0$. Finally $\bar{x}$ is Lyapunov stable.

As a conclusion, under appropriate conditions on u_{min} and u_{max}, the last main result of this section can be presented:

Theorem 10. With $u_{min} \leq \bar{x}_2/(\bar{x}_2 + \beta_2)$ and $u_{max} \geq \bar{x}_2/(\bar{x}_2 - \alpha_2)$, the fixed point $\bar{x}$ of (1) is globally asymptotically stable.

This last theorem is a simple corollary of Theorem 2 and Theorem 4.

A simulation of this control strategy applied to the calibration of the system used in Lugagne et al. (2017) is presented in Fig. 3. The multiplication by $u_{max} = 3$ of the reference control $u_1 = 0.25$ is equivalent to reducing the aTc dose to $6.5\text{ng} \cdot \text{ml}^{-1}$. Similarly, the multiplication by $u_{min} = 0.27$ of the reference control $u_1 = 0.25$ is equivalent to increasing the aTc dose to $42.9\text{ng} \cdot \text{ml}^{-1}$. It can be observed that the switch between $\text{aTc} = 6.5\text{ng} \cdot \text{ml}^{-1}$ and $\text{aTc} = 42.9\text{ng} \cdot \text{ml}^{-1}$ leads to a stabilization of $\bar{x}$, as analytically predicted. This control strategy may lead to a simplification of the experimental set-ups as it only needs one measurement system for *lacI* and one inducer molecule aTc. Moreover, the global results are still valid if u_{min} and u_{max} vary, as long as they verify the conditions stated in Theorem 10. In other words, if the low dose of

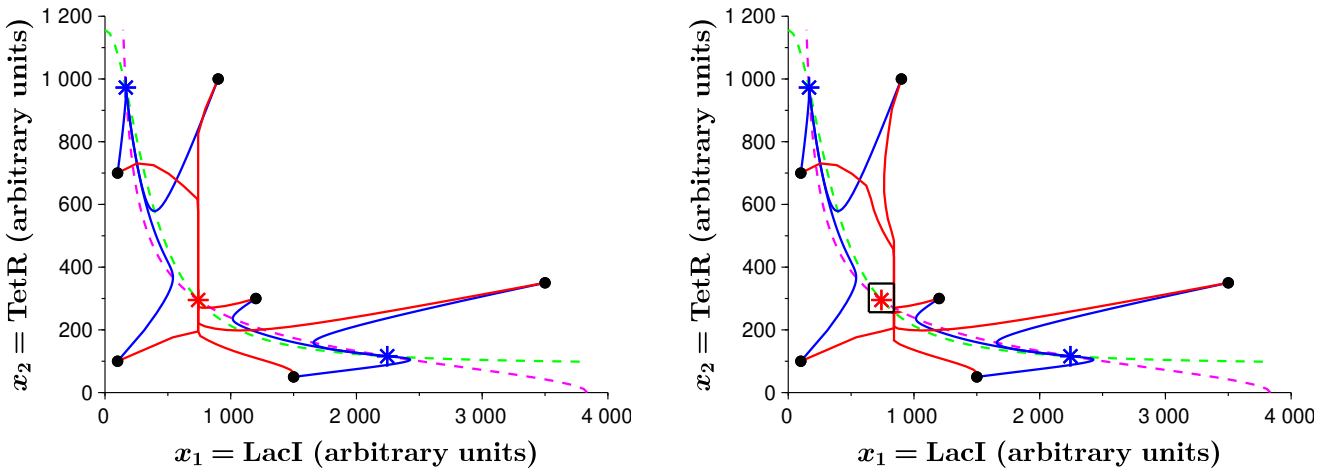

Fig. 3. For both plots: parameters are the one in table 1, the pink (resp. green) dashed line is the x_1 (resp. x_2) nullcline of (1), the blue stars are the stable fixed points, the red star the unstable fixed point, the blue lines are simulations of the uncontrolled system with six initial conditions depicted with black dots. Left: the red lines are simulations of (2) with a switch between $\text{aTc} = 6.5\text{ng} \cdot \text{ml}^{-1}$ and $\text{aTc} = 42.9\text{ng} \cdot \text{ml}^{-1}$. Right: The red lines are simulations of (3) with $E = 100$. The black square is the convergence region.

aTc is smaller than $6.5\text{ng} \cdot \text{ml}^{-1}$ (it can even be 0) and the upper dose greater than $42.9\text{ng} \cdot \text{ml}^{-1}$, the convergence is guaranteed. This property allows fluctuations in the doses of aTc.

5. UNCERTAIN MEASUREMENTS

The major drawback of this control strategy is its sharp dependence on the detection of the frontier $\bar{x}$. As soon as measurement devices display an uncertainty range, the strict convergence towards $\bar{x}_1$ is not guaranteed any more. The imperfect measurement device is supposed to present a range of uncertainty of length $2E$ (Mairet and Gouzé, 2016): in other words, for a measured x_1, the real system might be anywhere in the range $[x_1 - E, x_1 + E]$. At the level of the control, (2) becomes:

$$\begin{aligned} \dot{x}_1 &= \kappa_{01} + \kappa_1 \text{h}^-(u(x_1)x_2, \theta_2, n_2) - \gamma_1 x_1, \\ \dot{x}_2 &= \kappa_{02} + \kappa_2 \text{h}^-(x_1, \theta_1, n_1) - \gamma_2 x_2, \end{aligned} \tag{3}$$

where $u(x_1) = u_{min} < 1$ if $x_1 \leq \bar{x}_1 - E$ and $u(x_1) = u_{max} > 1$ if $x_1 \geq \bar{x}_1 + E$. When $x_1 \in]\bar{x}_1 - E, \bar{x}_1 + E[$, the control is undetermined and may take either u_{min} or u_{max} without any specific transition law or probability distribution.

Initially it is assumed that E is small enough for simplicity:

Assumption 11. The uncertainty length E verifies: $0 < E < \min(\bar{x}_1 - \kappa_{01}/\gamma_1, (\kappa_{01} + \kappa_1)/\gamma_1 - \bar{x}_1)$.

Similarly to what was done in Section 4, under Assumption 11 the space is partitioned in 5^2 zones $(a_1 a_2)$:

Definition 12. For $i \in \{1, 2\}$:

- $a_i = 0$ if $x_i < \bar{x}_i - \alpha_i$,
- $a_i = 1$ if $\bar{x}_i - \alpha_i \leq x_i < \bar{x}_i - \omega_i$,
- $a_i = 2$ if $\bar{x}_i - \omega_i \leq x_i \leq \bar{x}_i + \lambda_i$,
- $a_i = 3$ if $\bar{x}_i + \lambda_i < x_i \leq \bar{x}_i + \beta_i$,
- $a_i = 4$ if $\bar{x}_i + \beta_i < x_i$,

where α_i and β_i are defined as in Definition 1, and

- $\lambda_1 = \omega_1 = E$,
- $\omega_2 = \bar{x}_2 - \frac{\kappa_{02} + \kappa_2 \text{h}^-(\bar{x}_1 + \lambda_1, \theta_1, n_1)}{\gamma_2}$,
- $\lambda_2 = \frac{\kappa_{02} + \kappa_2 \text{h}^-(\bar{x}_1 - \omega_1, \theta_1, n_1)}{\gamma_2} - \bar{x}_2$.

It is easy to check that $\kappa_{01}/\gamma_1 = \bar{x}_1 - \alpha_1 < \bar{x}_1 - \omega_1 < \bar{x}_1 < \bar{x}_1 + \lambda_1 < \bar{x}_1 + \beta_1 = (\kappa_{01} + \kappa_1)/\gamma_1$ and $\kappa_{02}/\gamma_2 < \bar{x}_2 - \alpha_2 < \bar{x}_2 - \omega_2 < \bar{x}_2 < \bar{x}_2 + \lambda_2 < \bar{x}_2 + \beta_2 < (\kappa_{01} + \kappa_1)/\gamma_1$.

This new partitioning allows the statement of the last main result of this paper:

Theorem 13. With $u_{min} \leq \bar{x}_2/(\bar{x}_2 + \beta_2)$ and $u_{max} \geq \bar{x}_2/(\bar{x}_2 - \alpha_2)$, (3) converges globally towards the zone (22).

The proof of this theorem follows exactly the same ideas as the one constructed for Theorem 2. Lemma 3 is fully valid for this new system: its proof is slightly modified by adapting the evaluation of the vector fields in the new regions. If E does not fulfill Assumption 11, results of Theorem 13 are still valid: if $E \geq (\kappa_{01} + \kappa_1)/\gamma_1 - \bar{x}_1$ (resp. $E \geq \bar{x}_1 - \kappa_{01}/\gamma_1$), from the natural bounds of (1), it is sufficient to define $\lambda_1 = \beta_1$ (resp. $\omega_1 = \alpha_1$). In this case, the regions $a_1 = 3$ and $a_2 = 1$ (resp. $a_1 = 1$ and $a_2 = 3$) do not exist, and the proof follows the same steps by skipping those about missing regions. The transition graph summarizing the construction of the proof is exactly the same as the one illustrated in Fig. 2.

Again, a simulation of this control strategy under uncertain measurements applied to the calibration of the system used in Lugagne et al. (2017) is presented in Fig. 3. It can be observed that with an uncertainty range of arbitrary length $2E = 2 \times 100$, the switch between $\text{aTc} = 6.5\text{ng} \cdot \text{ml}^{-1}$ and $\text{aTc} = 42.9\text{ng} \cdot \text{ml}^{-1}$ leads to a stabilization of the zone $\{x_1 \in [\bar{x}_1 - 100, \bar{x}_1 + 100], x_2 \in [\bar{x}_2 - 39, \bar{x}_2 + 52.6]\}$, as analytically predicted. Simulations need a probability distribution for the control in the region $a_1 = 2$ as it may take any of the two values u_{min} and u_{max}. As no a priori probability is evident about fluctuations in the measurements, the numerical results are presented here with a

classic discrete uniform distribution where the probability for u_{min} and u_{max} is the same. Obviously, the analytical convergence result does not depend on this probability distribution choice.

This control strategy is able to guarantee a zone of convergence around $\bar{x}$ when measurements are not perfect. This result is satisfactory as a strict convergence towards $\bar{x}$ would not have any importance if the measurement device was not able to detect it. Moreover, when the uncertainty range decreases, the convergence zone (22) shrinks around $\bar{x}$. This gives an indication on the measurement device performance needed for a given desired convergence zone.

Unfortunately, this control strategy has the disadvantage of switching relatively quickly between u_{min} and u_{max}, meaning that in the biological context, the introduction and the removal of aTc must be fast as well. However, removing an inducer molecule from a biological system is not an easy task. To address this issue, optogenetic techniques might be a good alternative to implement this control strategy in the context of the Toggle Switch presented in Lugagne et al. (2017). Indeed, *lacI* is repressed by an homodimer of TetR and biologists have tools to create photosensitive homodimers that are able to dissociate after being exposed to light (Chen et al., 2013). Moreover, optogenetics is able to mimic this on-off type approach and is known to be fast, non-invasive, and well targeted.

6. CONCLUSION

This paper highlighted a control strategy for the stabilization of the unstable fixed point of genetic positive feedback loops. Biological measurements and control constraints encouraged the use of hybrid systems with piecewise constant control laws. By measuring and controlling only one of the two genes, this new control strategy leaded to interesting global results. First, the global convergence was proved by partitioning the state space into repelling regions. Second, the Lyapunov stability was verified by constructing specific nested balls in which trajectories were trapped, providing robustness. Finally, a small zone of convergence was highlighted under the hypothesis of uncertain measurements, validating this control under more realistic conditions. Importantly this new control strategy suggests that biological implementations in Lugagne et al. (2017) where two controls and two measurements are needed, may be reduced to a unique measurement and a unique control for an equivalent result.

A major advantage of this control strategy is that it may be applied to systems of any dimension N and can then be implemented for other biological positive feedback loops (Brandman et al., 2005): our current work focuses on this generalization. However, this model does not take into account cells inherent stochasticity. A natural extension of this work would be to include a stochasticity version of cell dynamics and adapt the control strategy in order to guarantee on average a convergence in a region around $\bar{x}$. Another major drawback of this work consists on assuming that the control can be changed as fast as possible, which is not realistic. A good start in order to tackle this problem would be to fix a delay during which control inputs could not be changed. This hypothesis would lead to the hard task of studying switched differential systems with discontinuous right hand sides (Lunze and Lamnabhi-Lagarrigue, 2009). Depending on the delay amplitude, a convergence zone around the fixed point might be determined. Finally, with these types of control, as soon as the inputs are removed, the system recovers its original behavior. A more viable strategy would be to modify intrinsically the genetic motif by either changing, removing or adding promoters within specific genes. These strategies are almost achievable nowadays thanks to synthetic biology.

REFERENCES

Brandman, O., Ferrell, J.E., Li, R., and Meyer, T. (2005). Interlinked fast and slow positive feedback loops drive reliable cell decisions. *Science*, 310(5747), 496–498.

Brette, R. and Gerstner, W. (2005). Adaptive exponential integrate-and-fire model as an effective description of neuronal activity. *Journal of neurophysiology*, 94(5), 3637–3642.

Cai, S., Fu, X., and Sheng, Z. (2007). Dedifferentiation: a new approach in stem cell research. *Bioscience*, 57(8), 655–662.

Casey, R., De Jong, H., and Gouzé, J.L. (2006). Piecewise-linear models of genetic regulatory networks: equilibria and their stability. *Journal of mathematical biology*, 52(1), 27–56.

Chaves, M. and Gouzé, J.L. (2011). Exact control of genetic networks in a qualitative framework: The bistable switch example. *Automatica*, 47, 1105–1112.

Chen, D., Gibson, E.S., and Kennedy, M.J. (2013). A light-triggered protein secretion system. *J Cell Biol*, 201(4), 631–640.

Farcot, E. and Gouzé, J.L. (2009). Periodic solutions of piecewise affine gene network models with non uniform decay rates: the case of a negative feedback loop. *Acta Biotheoretica*, 57, 429–455.

Fracassi, C., Postiglione, L., Fiore, G., and Di Bernardo, D. (2015). Automatic control of gene expression in mammalian cells. *ACS synthetic biology*, 5(4), 296–302.

Gardner, T.S., Cantor, C.R., and Collins, J.J. (2000). Construction of a genetic toggle switch in Escherichia coli. *Nature*, 403(6767), 339.

Lugagne, J.B., Sosa Carrillo, S., Kirch, M., Köhler, A., Batt, G., and Hersen, P. (2017). Balancing a genetic toggle switch by real-time feedback control and periodic forcing. *Nature Communications*, 8, 1671.

Lunze, J. and Lamnabhi-Lagarrigue, F. (2009). *Handbook of hybrid systems control: theory, tools, applications*. Cambridge University Press.

Mairet, F. and Gouzé, J.L. (2016). Hybrid control of a bioreactor with quantized measurements. *IEEE Transactions on automatic control*, 61(5), 1385–1390.

Milias-Argeitis, A., Rullan, M., Aoki, S.K., Buchmann, P., and Khammash, M. (2016). Automated optogenetic feedback control for precise and robust regulation of gene expression and cell growth. *Nature communications*, 7, 12546.

Purcell, O., Savery, N.J., Grierson, C.S., and Di Bernardo, M. (2010). A comparative analysis of synthetic genetic oscillators. *Journal of the Royal Society Interface*, 7, 1503–1524.